Single-molecule electronic materials. Conductance of π-conjugated oligomers within quasi-correlated tight-binding model

A.V.Luzanov

SSI "Institute of Single Crystals", National Academy of Sciences of Ukraine, 60 Nauky Ave., 61001 Kharkiv, Ukraine

For computing electric conductance through organic nanowire of conjugated type we make use of the recently proposed quasi-correlated tight-binding (QCTB) method. The appropriate Green's function (GF) matrices are constructed, and simple numerical algorithms are given for them. Moreover, the GF analytical solutions are obtained for finite-sized polyene chains and other systems. A special attention is paid to conjugated oligomers with various strength of electron correlation. In particular, we find that in polyquinoids the conventional Huckel and restricted Hartree-Fock methods lead, in contrast to QCTB, to a nonphysical increase of GF matrix elements for far separate contacts.

Keywords: single-molecule conductance, Green's function, quantum interference, π-electron correlation, conjugated oligomers.

Для вычислений электрической проводимости через органический нанопровод сопряженного типа введен квазикорреляционный метод сильной связи (QCTB). Построены соответствующие матрицы функции Грина (GF) и разработаны несложные вычисленные схемы. Получены аналитические выражения для GF конечных полиеновых цепочек и других систем. Особенное внимание уделено сопряженным олигомерам с различной степенью электронной корреляции. В частности, обнаружено, что в полихиноидах стандартная схема по Хюккелю и ограниченный метод Хартри-Фока приводят, в отличие от QCTB, к нефизичному возрастанию элементов GF отдалённых контактов.

Електронні матеріали з окремих молекул. Провідність π-супряжених олігомерів на засадах квазікореляційного методу сильного зв'язку. *А.В.Лузанов.*

Для обчислень електричної провідності через органічний нанодріт супряженого типу впроваджено квазікореляційний метод сильного зв'язку (QCTB). Побудовано відповідні матриці функції Грину (GF) та розроблено нескладні обчислювальні схеми. Крім цього, отримано аналітичні вирази GF стосовно кінцевих полієнових ланцюжків та інших систем. Особливу увагу приділено супряженим олігомерам із різною силою електронної кореляції. Зокрема знайдено, що у поліхіноїдах стандартна схема за Хюккелем та обмежений гартрі-фоківський метод ведуть, на відміну від QCTB, до нефізичного зростання елементів GF віддалених контактів.

1. Introduction

The phenomenon of single molecule conductivity has attracted considerable interest in condensed matter physics and material science from both theoretical and applied points of view [1–4]. The quantum conduc-tance theory of metal-molecule-metal (mMm) junction is primarily based on the nonequilibrium Green's function (GF) technique described in details in [1, 5, 6]. In this field various customary quantum chemistry models are frequently applied. Typical are one-electron semiempirical calculations

of GF from which the conventional electron transmission through mMm junction can be easily studied. The most popular remain one-electron Huckel-like schemes that provide the tight-binding (TB) approximation for valent π-electrons (see the most up-to-date review [7]). However, some vital problems had not yet been subject to adequate consideration. The key issue here is whether the Huckel model is sufficiently reliable, at least qualitatively, for finding GF, especially in extended systems. Evidently, a comprehensive answer to this issue cannot be given in advance, and it motivated us to make an appropriate comparative analysis staying within the limits of current π-electron theories. Previous studies in the same line, particularly in [8, 9], also support an argument for more research in this topic.

It would be no less important to suggest electron-correlation models which could simply and easily be implemented for computing mMm junction conductance in the case of sufficiently large conjugated molecules. In the present paper the quasi-correlated tight-binding (QCTB) approximation from [10−12] is proposed for this purpose. The method we are developing here is applied to typical π-conjugated oligomers and to strongly correlated π-systems such as non-Kekulean hydrocarbons.

2. Molecular conductance in a simplest one-electron scheme

We start with notations and definitions. Within conventional theories of ballistic electron transport through molecule the fundamental magnitude is the electric conductance, g_{ab}, for the given molecule coupled to two current-carrying metal leads a and b. The given mMm junction will be termed the $a−b$ connection. In the present paper we will deal with π-conjugated systems only, and we may use the same symbols a and b for the π-orbitals coupled with the respective leads. Then, the commonly used relation for the conductance is of the form [1]

$$g_{ab}/g_0 = 4\Gamma_a\Gamma_b|G_{ab}|^2, \qquad (1)$$

where G_{ab} is (a,b) matrix element of an one-electron retarded GF for π-system, and g_0 is the quantum conductance unit. Furthermore, phenomenological parameters Γ_a and Γ_b appear in Eq. (1) as a result of the so-called wide-band approximation (WBA) [1] (see also [13−15]). They represent an effect of broading energy levels due to coupling the mole-

cule to lead contacts. In the paper, $a−b$ connections by the same-type leads will be only considered, so we put $\Gamma_a = \Gamma_b \equiv \Gamma$.

The retarded GF matrix, G, is the key matrix of any consistent quantum theory of molecular conductance, and this GF is the main concern of the present paper too. Generally, GF is energy dependent matrix: $G = G(E)$. In the simple TB approximation we work with the conventional one-electron Hamiltonian matrix h^0 defined in a π-AO basis. For bipartite (alternant) hydrocarbons, we can always represent h^0 as a skew-diagonal block matrix of the form

$$h_0 = -\begin{pmatrix} 0 & B \\ B^+ & 0 \end{pmatrix}, \qquad (2)$$

where B describes interactions between "starred" and "unstarred" cites only (the latter are taken from two disjoint carbon atom sets). In our case it is pertinent to think about B as a matrix composed of one and the same elements $|\beta_0|$ is the CC bond resonance integral) for any pair of connected carbon atoms. Other elements of B are zero by definition; for more detail we refer the reader to [16].

At this TB level, we compute the standard GF as an usual matrix resolvent of h^0. But the above mentioned broading of energy levels should be additionally involved in an effective molecular GF of mMm junction. Throughout the paper the simplest WBA scheme from [13, 14] will be employed by using, instead of a full tunneling-width matrix, the one-parametric diagonal matrix $(i\Gamma)I$ where I is the identity matrix of appropriate order. The final expression used in our TB computations of GF is

$$G^{TB} = [(E + i\Gamma)I - h_0]^{-1}. \qquad (3)$$

From now on, we will apply a suitable shorter notation:

$$G^{TB}(z) = (z - h^0)^{-1}, \qquad (3')$$

where a complex energy z is equal to

$$\tilde{E} = E + i\Gamma. \qquad (4)$$

Moreover, the identity matrix is not explicitly written, that is $z \equiv zI$ in all matrix expressions here and elsewhere. It is necessary to stress again that the TB Huckel scheme may be too crude for computing GF, as will be seen from many examples.
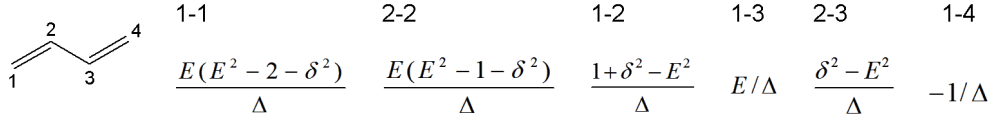
	1-1	2-2	1-2	1-3	2-3	1-4
	$\dfrac{E(E^2-2-\delta^2)}{\Delta}$	$\dfrac{E(E^2-1-\delta^2)}{\Delta}$	$\dfrac{1+\delta^2-E^2}{\Delta}$	E/Δ	$\dfrac{\delta^2-E^2}{\Delta}$	$-1/\Delta$

Fig. 1. GF elements within QCTB for connections 1–1, 2–2 etc. in the $1/|\beta_0|$ units for; $\Delta = \Delta_4$ is given by Eq. (10).

3. Green's function for QCTB

We initially outline basic points of the QCTB method which was elaborated before in [10–12] for analyzing electron correlation in spin-singlet π-electron structures. Instead of the initial Hamiltonian h^0, Eq. (2), we need to define two one-electron Hamiltonians. These are

$$h^\alpha = -\begin{pmatrix} \delta & B \\ B^+ & -\delta \end{pmatrix}, \quad h^\beta = -\begin{pmatrix} -\delta & B \\ B^+ & \delta \end{pmatrix}, \qquad (5)$$

where in matrix expressions $\delta \equiv \delta I$, and a number δ is a spin orbital splitting parameter. By the latter we introduce spin-polarization effects as a crude model of the π-electron correlation caused by the inter-electronic (Coulomb) repulsion.

Now we turn to our problem. Starting from the above Hamiltonians one can easily construct the corresponding GF matrices of the type (3). But only their symmetric combination has a sense for spin-singlet states. It leads us to the following GF definition at the QCTB level (for spin-singlet states):

$$G^{\mathrm{QCTB}}(\tilde{E}) = \frac{(\tilde{E} - h^\alpha)^{-1} + (\tilde{E} - h^\beta)^{-1}}{2}. \qquad (6)$$

Thanks to the specific block-matrix structure of Eq. (5), we can reduce Eq. (6) to the equivalent compact form

$$G^{\mathrm{QCTB}}(\tilde{E}) = \frac{\tilde{E} + h^0}{\tilde{E}^2 - \delta^2 - (h^0)^2} \qquad (7)$$

(the proof is given in Appendix A).

Here we give only one simple result ensuing from Eq. (7). Usually, the most interesting point on the energy scale is the Fermi level E_F (in fact E_F is the reference point on this scale). In case of the Hamiltonians in Eqs. (2) and (5), $E_F = 0$ and this value will be used in our TB and QCTB computations. Let us compare the corresponding GF at $E_F = 0$ that is matrix $G(0)$:

$$G^{\mathrm{TB}}(0) = -(h^0)^{-1}, \qquad (8)$$

and

$$G^{\mathrm{QCTB}}(0) = \frac{-h^0}{\delta^2 + (h^0)^2}. \qquad (9)$$

We see that in the case of singular TB Hamiltonian (then h^0 has zero eigenvalues), $G^{\mathrm{TB}}(0)$ is not correctly defined (while, more precisely, we must work with $G^{\mathrm{TB}}(i0^+)$, see section 7). At any rate, the TB π-orbital energy spectrum may be not correct, especially for large-scale π-conjugated networks, and it can entail problems in computing and interpreting G^{TB}. Unlike the TB method, in QCTB the TB zero-energy eigenvalues or almost-zero-energy TB-eigenvalues are removed due to the nonnull δ, and this gives us the correctly defined $G^{\mathrm{QCTB}}(0)$, as seen from Eq. (9). Notice that in practical computations we use, as previously in [10–12], $\delta = 7/24$ (in the $|\beta_0|$ units).

4. Short polyene chains

We will study here two models of linear polyenes: regular chains and bond alternated chains. The regular polyene chain with identical CC bond lengths is a paradigmatic for the analytical consideration of spectral TB problems (see any textbook on quantum chemistry). For the same regular chain, the required expression for G^{TB} was furnished long ago in [17] within the related chain-vibration theory. However, more appropriate representations of G^{TB} were given afterwards in [18–21]. Based on their finding, the G^{QCTB} full analytical results can be easily obtained via Eqs. (6) and (7) in form of Eqs. (B7)–(B10) of Appendix B.

Below we first revisit the example of the butadiene molecule which is frequently analyzed in the literature [7, 8, 21–23]. The corresponding QCTB expressions obtained from Eqs. (B7)–(B10), turn out to be indicative of the general situation (Fig. 1).

In Fig. 1 we denote by $\Delta = \Delta_4$ a secular determinant of the QCTB problem for butadiene:

$$\Delta_4 = 1 - 3(E^2 - \delta^2) + (E^2 - \delta^2)^2. \qquad (10)$$

If needed, E in the above can be replaced with $\tilde{E}$ Eq. (4). Considering the case of $\delta = 0$, we return to the usual secular TB deter-

minant $\Delta_4 = 1 - 3E^2 + E^4$, which has the known roots (gold ratio number $(1 + \sqrt{5})/2$ and others). It is thus no wonder that these roots (the TB orbital energies in the $|\beta_0|$ units) are the same E values at which the conductance peaks occur. Of course, this is the well known fact (e.g., see Fig. 3 in [22]). Less evident is why the GF nodes (antiresonances in terms of [24]) occur as well. By definition, antiresonances are zeros of electron transmission, that is, the E values at which the molecular conductance disappears or becomes very small. It is the so-called destructive quantum interference. In case of the butadiene molecule we see from Fig. (1) that for $\delta = 0$ the antiresonances occur at $E = \pm 1$ and $E = \pm\sqrt{2}$. To better understand the causes for this, we consider analytical results for polyene chains in a suitable form of Eqs. (B2)–(B8). In particular, for the butadiene we have

$$G_{*o}^{TB}(E) = \frac{1}{\Delta_4}\begin{pmatrix} \Delta_3 & 1 \\ 1 & \Delta_1\Delta_2 \end{pmatrix} \qquad (11)$$

with $\Delta_1 = -E$, $\Delta_2 = 1 - E^2$, and $\Delta_3 = -E(2 - E^2)$. Now recall that for the given k, Δ_k is the TB (Huckel) secular determinant for the k-atomic polyene chain (recall Eq. (B1) in Appendix B). Hence, the antiresonances, for instance in the butadiene, correspond to orbital energies of the allylic and ethylenic fragments (besides, a free atom center with its own $\Delta_1 = -E$). Analogously, one can analyze $G_{*o}^{QCTB}(E)$. We now see that the GF matrix elements are factorized to be corresponding to the polyene subsystems, i.e., shorter chains [e. g., see Eqs. (B2) and (B3)]. This previously not well highlighted fact is apparently not accidental. At least, there is a nontrivial theorem due to Barrett stating that elements of inverse of tridiagonal matrices are all factorizable [25]. It is an interesting issue which is worth discussing separately. Notice the related study [26] in which coupled subsystems are analyzed. In moving to QCTB, the structure of Eq. (11) is preserved; only Δ_4 etc. are replaced by their QCTB counterparts (by Eq. (10) etc.), so that the positions of resonances and antiresonances are shifted approximately by $\delta^2/2$ for small δ.

Additional effects arise when taking into account a bond alternation in the polyene chain. In this case we must invoke the appropriate parameter $\tau = \beta_{C-C}/\beta_{C=C}$, a ration

of single and double bond resonance π-integrals. For the most important GF elements the analytical results are derived in Appendix B [see Eq. (B11)]. To be more specific, consider, say, G_{14}^{QCTB} in Eq. (B14) for the butadiene molecule. In the case of small values of E, δ, and a small alternation measure $1 - \tau$, we find that $G_{1,4}^{QCTB} = -[\tau + (5\tau - 2)(E^2 - \delta^2)]$. For $E = 0$ we have $G_{1,4}^{QCTB} = -\tau(1 - 5\delta^2)$, so that an inclusion of bond alternation and correlation effects (via δ) leads to a cooperative effect of lessening of G_{14}^{QCTB} (recall that $0 < \tau \leq 1$).

In the above examples QCTB makes only comparably small quantitative correction to the TB results. However, there are exist situations where electron correlation and other electronic effects may significantly influence even the qualitative behavior of molecular conductance, and in our example of the butadiene molecule we encounter this issue. Really, when analyzing the conductance through allowed channel 2–3, we observe in Fig. 1 that at $E = 0$ the 2–3 connection is locked within the TB scheme. In terms of [7] this is an example of the GF "hard zeros". Nonetheless, as seen from Fig. 1, QCTB permits the electric current through the 2–3 connection. In Fig. 1 we did not take account for bond alternation, but if doing that (see the last points in Appendix B) we will find from Eq. (B14) that G_{23}^{QCTB} does not vanish at $E = 0$ anyway, and it is approximately equal to $\tau\delta^2$. Hence, if used more advanced π-schemes, the above-mentioned hard zero turns out to be rather small but not exactly zero. In the next sections we get confirmation of these simple QCTB regularities.

5. Comparison with more exact approaches

We make now comparisons between TB, QCTB, and π-electron full configurational interaction (FCI) method. This method should be treated as the most rigorous π-approach. In its consistent form, π-FCI was presented in [27], and then extended in many works. We follow the π-FCI matrix formulation given in [28, 29]. All our FCI computations were made using this technique along with an auxiliary one from [30] which is inevitably required for finding the Dyson amplitudes. The latter are one of the building blocks of GF computations at the

FCI level (e.g., see Eq. (1) and the next relations in [9]).

In calculations of effective GF and conductance spectra we made using broading parameter $\Gamma = 0.05$ eV in agreement with [9]. In all the plots we show conductance (in the g_0 units) spectra for g_{ab} as a function of energy argument E and make using the logarithmic ordinate. Moreover, in all tables and figures, the specific connections are shown by stars and cycles; the spectra are plotted for the various π-models in this way: FCI (in red), QCTB (in green), and TB (black dashed).

Few words about the π-parameters we employ in the numerical calculations. In case of the polyenes and other structures with alternating bond lengths we use the TB Hamiltonian with parameter $\tau = 11/13$, so that $\beta_{C-C} = 11/12\beta_0$ and $\beta_{C=C} = 13/12\beta_0$, with $\beta_0 = -2.4$ eV being the adopted resonance integral of the aromatic π-bond (this alternation scheme was taken from [31]). The same parameters will be used in π-computations within FCI and restricted Hartree-Fock (RHF) schemes.

Another special point is how to compare the TB and QCTB data with those of RHF and FCI. The case of the ethylene molecule helps us to understand the problem. Indeed, for this two π-electron molecule the nondiagonal (1,2) element of h^0 is β_0 in TB, and that of the RHF effective Hamiltonian (Fockian) is equal to $\beta_{eff} = \beta_0 - \gamma_{12}/2$. Here γ_{12} is the Coulomb two-center repulsion integral for the nearest two sites (we adopt $\gamma_{12} = 7.553$ eV). The TB and RHF values of G_{12}, $1/\beta_0$ and $1/\beta_{eff}$, respectively, significantly differ each other (in eV^{-1}, $-1/2.4$ and $-1/6.18$, respectively). Almost the same value $1/\beta_{eff}$ is obtained for G_{12} in π-FCI; a similar picture is observed in most other examples. To minimize an inevitable gap between different approaches we rescale by factor $\beta_0/\beta_{eff} \equiv 0.3886$ all RHF and FCI values of the GF matrices. An analogous problem encountered earlier when compared the TB (Huckel) and RHF energies [32]. In all tables for RHF and FCI we give such rescaled GF elements. In doing so it is worth bearing in mind that after rescaling, $G_{1,2}^{TB} = G_{1,2}^{RHF}$ in the ethylene molecule. By passing, notice that no changes in the geometrical parameters were done when we performed computations for the polyenic systems with alternated bond lengths — only the above given alternation of resonance integrals was made.

In Table 1 we show the results for π-systems of the butadiene, C_4H_6, and decapentaene $C_{10}H_{12}$ molecules. We notice at once that qualitatively the results for $C_{10}H_{12}$ are quite similar to those of C_4H_6. In Table 1, the results for the closest 2–3 connection in C_4H_6 are additionally given. In the case of this 2–3 connection we find that the respective FCI picture is in fact the same as that predicted by QCTB in the previous section.
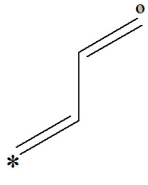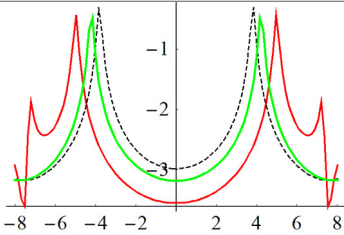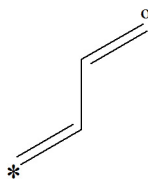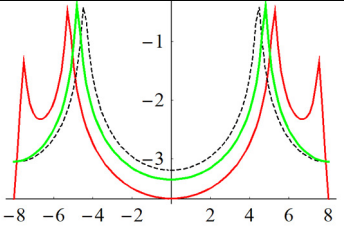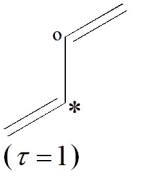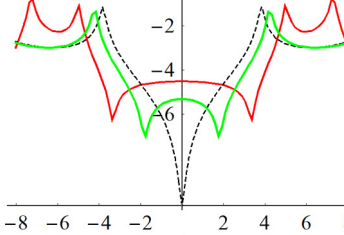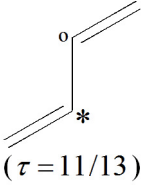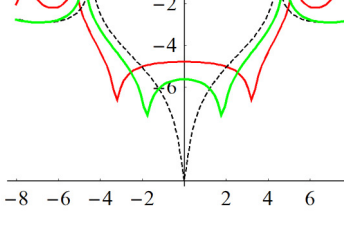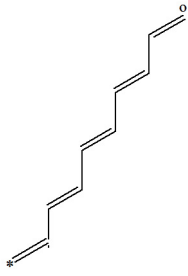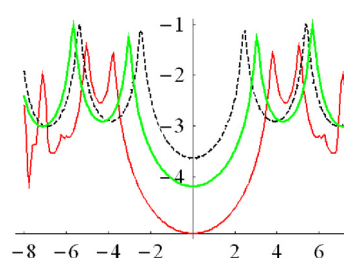
Our results for the 2–3 connection in C_4H_6 have some common features with those for the cross-conjugated model systems explored in [8]. In the cited work the antiresonances disappeared when the second and third order interactions are added to the topological matrix B. (see Fig. 6 in [81]). Stress again that even at the QCTB level the π-electron correlation comes to the same effect. In other words, there are no GF "hard zeros" at the FCI and even RHF level too. Remark that in the adopted π-parametrization for the bond-alternated polyenes we must multiply elements $[G_{*O}^{TB}(0)$ in Eq. (B13) by 12/11 in order to obtain the needed values (in the $|\beta_0|$ units) given in Table 1.

In whole, QCTB provides a qualitatively good data whereas there are the marked, sometimes large, quantitative deviations between QCTB and FCI (recall a logarithmic ordinate axis scale in the plots). With increasing $|E|$ values, the TB model as well as QCTB are numerically further away from the exact π-FCI theory. Naturally, simple approaches which ignore many-center interactions, come at a price. That is why RHF can (but not always, of course) provide a better picture than QCTB. Concurrently, we see an insignificant difference between QCTB and TB for sufficiently large E. This feature becomes transparent when comparing Eqs. (A6) and (A7) with Eq. (3), and recalling that δ is small in practice ($\delta^2 \cong 0.1$).

6. Chain-like π-electronic molecular wires

In this section we study GF in sufficiently large molecular wires based on several typical conjugated oligomers: polyenes, polyacenes, polyperylenes and polyxylylenes. They are displayed in Fig. 2, and labeled by **I**, **II**, **III**, and **IV**, respectively. In this figure by "o" we signify the position of the left-attached electrode, and by the numbered star symbols 1,2, ,…, ν_*, the possible

Table 1. Conductance spectra and the G_{*O} matrix elements at $E = 0$ within the various approaches for regular ($\tau = 1$) and alternating ($\tau = 11/13$) polyene molecules

Structure	Conductance spectrum	G_{*o}^{FCI}	G_{*o}^{RHF}	G_{*o}^{QCTB}	G_{*o}^{TB}
($\tau = 1$)		-0.518	-0.603	-0.792	-1.000
($\tau = 11/13$)		-0.447	-0.509	-0.649	-0.781
($\tau = 1$)		0.170	0.102	0.068	0.000
($\tau = 11/13$)		0.124	0.084	0.047	0.
($\tau = 11/13$)		0.086	0.097	0.250	0.472

positions of the right-attached electrode (ν denotes the maximal number of the considered contact pairs). Furthermore, the selected pairs o-1, o-2, etc. are just the connections which are allowed by the known selection rule (A10). At once we will notice that usual long-distance effects should be decreasing with distance. Hence, it seems reasonable to expect vanishing of matrix elements G_{ab} for too far separated π-atomic centers a and b. Failure to implement these natural expectations means, in fact, an un-
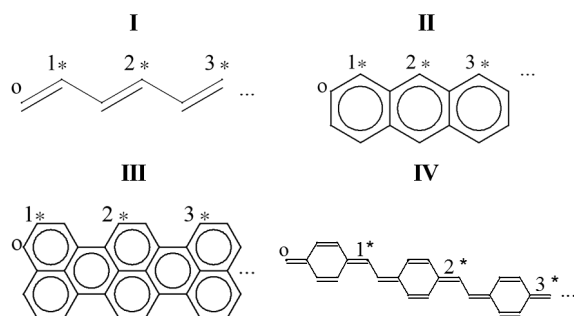
Fig. 2. Chemical formulae of the main studied systems.

suitable model for molecular conductance effects. For our computations, we took the systems from Fig. 2 with $\nu = 10$ for **I** and **II**, and $\nu = 9$ for **III** and **IV**.

The obtained results are given in plots of Fig. 3. In the plots we exhibit the dependency of $G_{o,k*}(0)$ on number k (in fact, an effective distance dependency) for oligomers **I–IV**. The results are based on the main three π-approximations: TB (dashed lines), QCTB (green lines), and RHF (blue lines). We start the discussion by the alternating bond polyene system $C_{20}H_{22}$ (**I** in Fig. 3). From Fig. 3 we see that qualitatively all the approximations do behave correctly, i. e., provide a systematic reduction of $\left|G_{o,k*}(0)\right|$ with increasing k. At the same time, quanti-

tatively the TB method shows a too slow decrease of $\left|G_{o,k*}(0)\right|$ in comparison with the more correct (at least in this case) QCTB and RHF models. The decacene molecule example (**II** in Fig. 3) yields a similar qualitative and only a little different quantitative picture.

For **III** and **IV**, a drastically different situation is observed. We see that the perylene oligomer **III** demonstrates the unnatural almost constant $\left|G_{o,k*}(0)\right|$ values within TB, unlike the well behaved values of the RHF and QCTB models. The last system **IV** gives a quite "pathological" increase of $\left|G_{o,k*}(0)\right|$ for large k in TB as well as in RHF. Only QCTB produces a reasonable picture for all the cases — that is gives a systematic decreasing $\left|G_{o,k*}(0)\right|$ (in the case of **IV**, the green line (QCTB) is almost merged with the abscissa for large k). We recognize that electron correlation plays a crucial role in large quinoid systems, so that TB and sometimes RHF are inapplicable even qualitatively in this case.

7. Peculiarities of non-Kekule structures

Particularly interesting is the case of singlet open-shell π-conjugated molecules. They represent a nice class of strongly correlated systems [33], which requires the high-level electron-structure theories. Nevertheless, as we will see now, some low-level
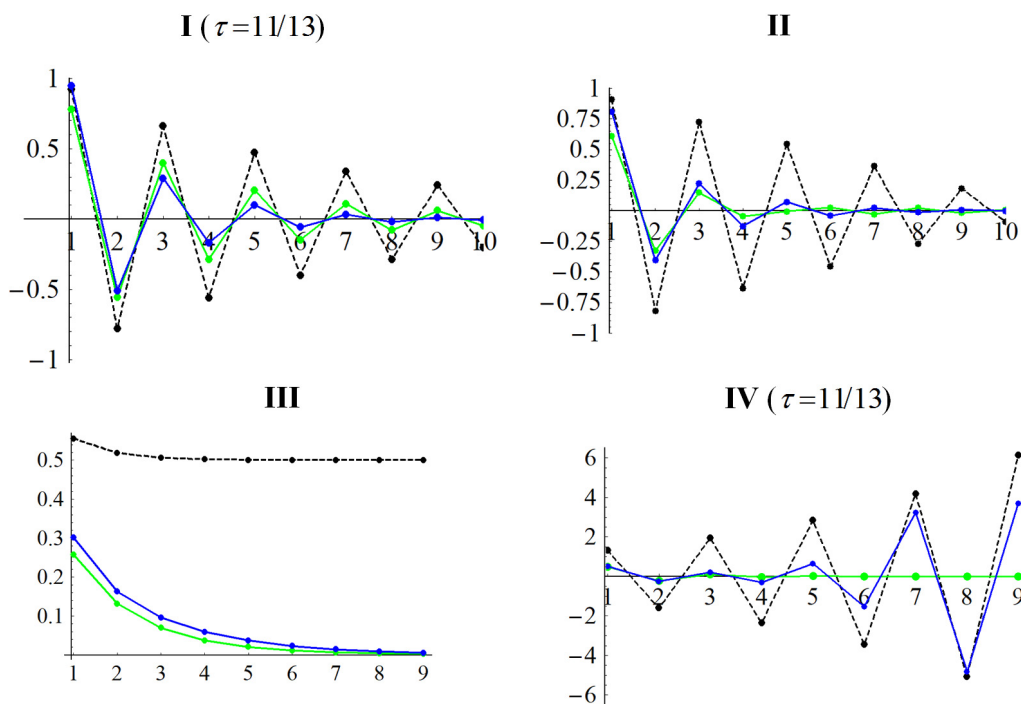

Fig. 3. Dependence of $G_{o,k*}(0)$ on "length" k for **I**, **II**, **III**, and **IV** from Fig. 2. The abscissa corresponds to k.

$$\begin{pmatrix} \dfrac{1}{2} & -\dfrac{1}{4} & -\dfrac{1}{4} \\ \dfrac{1}{2} & -\dfrac{1}{4} & -\dfrac{1}{4} \\ 0 & \dfrac{1}{2} & \dfrac{1}{2} \end{pmatrix} \qquad \begin{pmatrix} 2+\delta^2 & -1 & -1 \\ 2+\delta^2 & -1 & -1 \\ \delta^2 & 2+\delta^2 & 2+\delta^2 \end{pmatrix} \Big/ \Delta$$
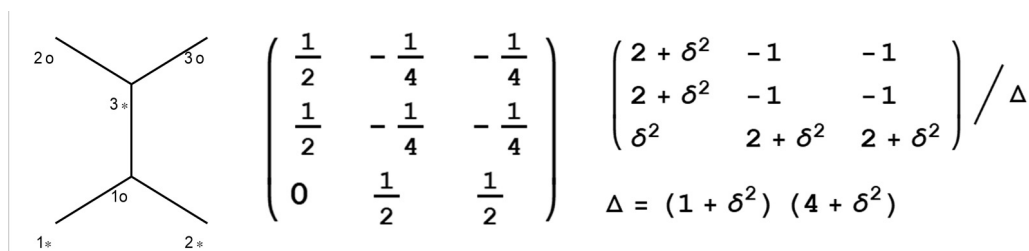
$$\Delta = (1+\delta^2)(4+\delta^2)$$

Fig. 4. The analytical GF blocks for TME within TB and QCTB.

models can be invoked as well at least for a crude simulation of the GF matrices.

Here we need to recall the one fundamental property of bipartites. Let us denote by n_* and n_o, respectively, a number of the corresponding starred and unstarred sites in the given bipartite. Then one can state that $S = (n_* - n_o)/2$ is a ground state total electron spin of this network. This is the remarkable Lieb rule which is exactly valid for FCI with the Hubbard Hamiltonian [34] (the analogous rule for valence bond models was given in [35]). Of course, the Lieb rule works for our bipartites as well. In particular, the system in Fig. 4 is the singlet molecule but with a diradical nature (open-shell singlet). The latter follows from the fact that this molecule is of the non-Kekule type (no Kekule structure can be drawn). Then $\det|h0| = (\det|B|)2 = 0$, (consult any chemical graph theory book, e.g. [16] for interrelation between $\det|h0|$ and a number of Kekule structures). Clearly, singlet non-Kekule molecules have nonbonding π-levels with orbital energies $\varepsilon j = EF = 0$, so $h0$ will be a rank-deficient matrix, and not conventionally invertible.

While the usual $(h^0)^{-1}$ does not exist in this case, the real part of GF at the Fermi level $G^{TB}(0)$ does. This is a result of the rigorous definition of the retarded GF. Namely, even thou we take $\Gamma = 0$, the retarded $G^{TB}(0)$ at $E = 0$ should be formally taken as $G^{TB}(i0^+) = (i0^+ - h^0)^{-1}$ where symbol 0^+ is conventionally understood as a passage to the limit $\gamma \to 0$. Then

$$G_{*O}^{TB}(0) = \mathrm{Re}[G_{*O}^{TB}(0)] = \tag{12}$$
$$= \lim_{\gamma \to 0}(\gamma^2 + BB^{T})^{-1}B.$$

Such matrices are directly related to the Moore-Penrose pseudoinverse (e.g., see theorem 3.4.1 in [36]). By the passage to the limit in Eq. (12) one removes the matrix singularity which occur due to nonbonding

MOs. Thus, at $E = 0$ we in fact calculate $G_{*O}^{TB}(0)$ as the pseudoinverse of B^{T}.

In addition, we describe below a simple algorithm for computer algebra systems, which allows us to construct the G^{TB} and G^{QCCT} analytical (explicit) expressions, in particular, for non-Kekule ("singular") structures. In our work, the specific results were obtained through the use of the software package Mathematica 5.2 [37].

The method is based on finite-step recursion for the matrix pseudoinversion procedure of type Hamilton-Cayley method (Eq. (5.4.2.1) in [36]). Such numerical computations were performed in quantum chemistry too, e. g., see [38]. In the algorithm, for the given matrix A, we generate a sequence of numbers $\xi^{(k)}$ and matrices $\sigma^{(k)}$, starting from $\xi^{(0)}$ and $\sigma^{(0)}$. The recursion is carried out as follows:

$$\sigma^{(k+1)} = \xi^{(k)} - A\sigma^k, \quad \xi^{(k+1)} = \frac{\mathrm{Tr}A\sigma^{(k+1)}}{k+1}, \tag{13}$$

where $k = 0, 1..., \rho - 1$, with ρ being a prescribed rank of A. Then the A pseudoinverse is of the form: $A^{\#} = \sigma^\rho / \xi^{(\rho)}$. When computing G_0^{QCCT} we make a choice: $A = \delta^2 + BB^T$ and $\rho = n_*$, so that $G_{O*}^{QCTB}(0) = BA^{\#}$, and for nonzero δ it will be a conventional full-rank inverse.

The above is a rather general scheme which is readily coded in the Mathematica language. In passing, we remark that matrix $G_{O*}^{TB}(0) = B^{\#}$ (then in Eq. (13) we put $A = BB^T$) provides a natural generalization of the Ruedenberg-Pauling bond orders for singular bipartite structures of non-Kekule type. As to the Ruedebgerg-Pauling bond orders see recent works [39−41].

As example of the simplest non-Kekule π-structure we consider the tetramethylene ethylene (TME) molecule — the needed blocks G_{*O} are presented in Fig. 4. Recall that in this figure $G_{*O}^{TB}(0)$ is matrix of the
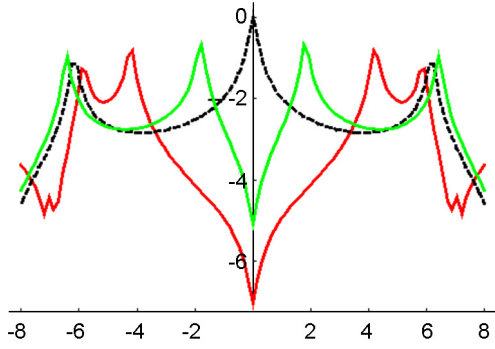
Fig. 5. TME conductance spectra for the "forbidden" 1_*-2_* connection within FCI (in red), QCTB (in green), and TB (in dashed black).

'singular' Ruedenberg bond orders (i. e., $G^{TB}_{*_*}(0) = B^{\#}$), rather than the usual one which does not exist for TME.

Note also that for usual (Kekulean) structures with zero HOMO-LUMO gaps the numerical pseudoinversion technique was discussed recently in [42].

From Fig. 4 we see that in the obtained QCTB matrix no singularity appears whatsoever, even when setting spin-splitting parameter $\delta = 0$ that returns us to the correct TB Green's function matrix. It is possible to get the same GF by setting from the very beginning $\delta = 0$ in Eq. (13), but choosing another rank $\rho \equiv n_* - 1$. Interestingly, within TB the above mentioned GF hard zero arises for TME too (for the allowed connection $1_* - 1$). But it also disappears if moving from TB to QCTB — then $0 \to \delta^2/\Delta$ in $G_{*\circ}$, as seen from Fig. 4 for $1_* - 3$.

We can demonstrate with the same TME example that there exist yet another TB quasi-singularities which are also eliminated by passing to QCTB. They appear owing to the imaginary part of the computed GF matrix. We recall that only the real part of GF is block skew-diagonal, as in Eq. (A10). Concurrently, the GF imaginary part at the Fermi level should be obtained from $G_0 \equiv G(i\Gamma)$, and the imaginary part is a block diagonal matrix:

$$\text{Im}[G_0] = \begin{pmatrix} G_{**} & 0 \\ 0 & G_{\circ\circ} \end{pmatrix}, \qquad (14)$$

(see Eqs. (A6)–(A8) for $\tilde{E} = i\Gamma$). It seems that this selection rule was not previously formulated.

A more careful analysis of Eq. (A8), provides evidence for an abnormal behavior of $\text{Im}[G_0]$ inherent to non-Kekule π-systems at
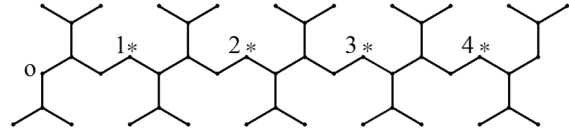

Fig. 6. The chemical structure of the allyl-decorated polyene chain with a high-order non-Kekulean character.

the TB level. To verify this, we compute GF for connection of the TME molecule, and show the results in Fig. 5. The obtained data are fully consistent with the expectations. Both QCTB and FCI confirm the artificial character of the G_0 singularity for non-Kekule structures. We see once again that QCTB provides a qualitatively reasonable picture of molecular conductance in a highly correlated system.

To conclude this section we suggest a new-type of non-Kekule structures. We will generate them from the polyene chains decorated by allylic groups, as seen in the example exhibited in Fig. 5. In such super non-Kekule systems we have, as previously, $n_* = n_\circ = N/2$, so the ground state spin should be the same: $S = 0$. But parallel to this, a number of nonbonding MOs is equal to the number of allylic groups, that is very large number for sufficiently long decorated chains. E.g., we have 10 nonbonding MOs for the system given in Fig. 6.

For the proposed non-Kekule structure, GF elements at the TB and QCTB levels are obtained without difficulties. We will discuss the special allowed connections $o-k_*$ shown on Fig. 6. It turns out that $G^{TB}_{o,k_*}(0) = -1$ for any k, that is within TB the GF values do not follow the pattern of long-distance vanishing (the same is in the initial polyene chain without bond alternation). Concurrently, for our super non-Kekule structure the more physical results are produced by QCTB:

$$G^{QCTB}_{0,k_*}(0)_{1 \leq k \leq 4} =$$

$$= -0.489, -0.241, -0.124, -0.073.$$

8. Conclusion

To summary, we stress again the principal need to use electron-correlation models for describing electronic transport through molecules. For this issue, it is not a simple matter to choose appropriately efficient and not time-expensive method applicable to large-scale molecular networks. Using the previously given QCTB scheme [10−12], the present paper proposes a rather crude but

very simple solution to the problem. In fact, we retain an elementary Huckel-type framework of the whole approach, and combine this with the simplest (one-parametric) spin-polarization model.

It allowed us to almost trivially construct Green's function matrices for any π-structures, even with zero TB orbital energy gap, for which the conventional Hartree-Fock method fails. The last two examples in Fig. 3 together with the unusual non-Kekule structures (Fig. 6), demonstrate wide-ranging possibilities of QCTB. It is also worth mentioning the obtained QCTB analytical expressions for polyene chains. At the same time, we cannot forget that QCTB is in fact a semiquantitative or even qualitative method for very large systems where long-range electronic effects might be essential. Subsequent studies will be able to clarify a real range of the QCTB applicability, and to explore further ways for improving our model. It is pertinent to note that QCTB was additionally applied in [45] for discussing the interesting effect of "spin repulsion" in alternant systems. Seemingly, the possibilities of QCTB are not exhausted by the previously treated problems of effectively unpaired electrons, as in [10−12], and by molecular electronics, as in the present work.

Acknowledgement. The paper is dedicated to the memory of Victor A.Kuprievich who 15 years ago called the author's attention to π-correlation problems in mMm junctions. The interesting discussion of the same subject with Hans Lischka also stimulated (with a lag) this paper.

Appendix A: Matrix partitioning technique for QCTB

Here we present suitable working expressions derived for GF by the conventional matrix partitioning technique. Of course, all the results below are valid for bipartites only. Let us first consider GF for spin-up electrons:

$$G^\alpha = (\tilde{E} - h^\alpha)^{-1}, \qquad (A1)$$

where h^α is given in Eq. (5). The block structure of h^α dictates $G^\alpha \equiv G^\alpha(\tilde{E})$ to be

$$G^\alpha = \begin{pmatrix} G^\alpha_{**} & G^\alpha_{*\circ} \\ G^\alpha_{\circ*} & G^\alpha_{\circ\circ} \end{pmatrix}. \qquad (A2)$$

Thus, for the given $\tilde{E}$ we must solve the matrix equation $(\tilde{E} - h^\alpha)G^\alpha = I$ for G^α of

the form (A2). After some algebra we get explicitly the individual blocks:

$$G^\alpha_{**} = (\tilde{E} - \delta)[\tilde{E}^2 - \delta^2 - BB^T]^{-1}, \qquad (A3)$$

$$G^\alpha_{\circ\circ} = (\tilde{E} + \delta)[\tilde{E}^2 - \delta^2 - B^TB]^{-1},$$

$$G^\alpha_{*\circ} = -(\tilde{E}^2 - \delta^2 - BB^T)^{-1}B, \qquad (A4)$$

The expressions for $G^\beta(\tilde{E}) = (\tilde{E} - h^\beta)^{-1}$ are obtained by replacing $\delta \to -\delta$ in Eq. (A3) and (A4); e. g., $G^\beta_{*\circ} = G^\alpha_{*\circ}$. All this leads to the correct (spin-symmetrized) GF given by Eq. (6):

$$G^{QCTB} = \frac{G^\alpha + G^\beta}{2} = \begin{pmatrix} G^{QCTB}_{**} & G^{QCTB}_{*\circ} \\ G^{QCTB}_{\circ*} & G^{QCTB}_{\circ\circ} \end{pmatrix}, \qquad (A5)$$

with the following submatrices:

$$G^{QCTB}_{**} = \tilde{E}(\tilde{E}^2 - \delta^2 - BB^T)^{-1}, \qquad (A6)$$

$$G^{QCTB}_{\circ\circ} = \tilde{E}(\tilde{E}^2 - \delta^2 - B^TB)^{-1},$$

$$G^{QCTB}_{*\circ} = -(\tilde{E}^2 - \delta^2 - BB^T)^{-1}B, \qquad (A7)$$

$$G^{QCTB}_{\circ*} = -B^T(\tilde{E}^2 - \delta^2 - BB^T)^{-1}.$$

When the spin-splitting parameter δ vanishes, these relations produce the TB solution:

$$G^{TB} = \begin{pmatrix} \tilde{E}(\tilde{E}^2 - BB^T)^{-1} & -(\tilde{E}^2 - BB^T)^{-1}B \\ -B^T(\tilde{E}^2 - BB^T)^{-1} & \tilde{E}(\tilde{E}^2 - BB^T)^{-1} \end{pmatrix}. \qquad (A8)$$

From the derived Eqs. (A6) and (A7) we will obtain useful rule for formal QCTB computations. We see by comparing Eqs. (A6) and (A7) with Eq. (A8) that the replacement

$$\tilde{E} \to \tilde{E}_\delta, \quad \tilde{E}_\delta \equiv \sqrt{E^2 - \delta^2} \qquad (A9)$$

should be done to produce the QCTB blocks G^{QCTB}_{**} and $G^{QCTB}_{*\circ}/\tilde{E}$ from the TB ones. Besides, from Eqs. (A5)−(A7) we find the G^{QCTB} eigenvalues, g_j, namely,

$$g_j = (\tilde{E} + \varepsilon_j)/(\tilde{E}^2 - \delta^2 - \varepsilon_j^2),$$

where ε_j are the TB orbital energies. It gives the explicit expression, Eq. (7), for G^{QCTB} in terms of h^0.

Another corollary from the above relations is the selection rules for G^{QCTB} at the Fermi energy, namely for the real part of GF we have the (more or less) known bipartite-symmetry selection rule:

$$\text{Re}[G(0)] = \begin{pmatrix} 0 & G_{*\circ} \\ G_{\circ*} & 0 \end{pmatrix}, \qquad \text{(A10)}$$

It trivially follows from Eqs. (A6) and (A7) for the QCTB block. As proved in [9], the rule of type (A10) holds for the most general (of course, correct) π-electron wave functions. Thus, the proposed QCTB model for GF works accurately in this regard.

Appendix B: Some analytical results for polyene chains

For our purposes we need renumbering the polyene chain sites in order to make the numeration consistent with Eqs. (A5) and (A8). Thus, instead of the consecutive numeration we will use numbers 1, 2,..., r, ..., n for the starred sites, and numbers n + 1, n + 2, ..., n + s, ..., n + n for the unstarred sites, and $n = N/2$. It allows us to rewrite the previously cited equations from [39, 40] for each submatrix in Eq. (A8), as follows. It is possible to associate with the k-atomic polyene chain the respective secular determinant $\Delta_k(z)$ as function of argument z, and express this in terms of the standard Chebyshev polynomial of the second kind, $U_k(z)$:

$$\Delta_k(z) = U_k(z/2). \qquad \text{(B1)}$$

Furthermore, we need to add the following three supplementary functions:

$$a_{rs}(z) = \Delta_{2r-2}(z)\Delta_{N+1-2s}(z)/\Delta_N(z), \qquad \text{(B2)}$$
$$b_{rs}(z) = -\Delta_{2r-2}(z)\Delta_{N-2s}(z)/\Delta_N(z),$$

$$c_{rs}(z) = -\Delta_{2s-1}(z)\Delta_{N-1-2r}(z)/\Delta_N(z). \qquad \text{(B3)}$$

Then the respective submatrices elements of the GF (A8), in the $|\beta_0|$ units, can be cast into the form ($r \le s$)

$$[G_{**}^{\text{TB}}(\tilde{E})]_{rs} = a_{rs}(\tilde{E}), \qquad \text{(B4)}$$
$$[G_{\circ\circ}^{\text{TB}}(\tilde{E})]_{rs} = a_{n-r+1,n-s+1}(\tilde{E}).$$

In so doing, $[G_{**}^{\text{TB}}(\tilde{E})]_{sr} = [G_{**}^{\text{TB}}(\tilde{E})]_{rs}$, and the same symmetry rule is for $G_{\circ\circ}^{\text{TB}}(E)$. Furthermore,

$$[G_{*\circ}^{\text{TB}}(\tilde{E})]_{rs} = b_{rs}(\tilde{E}), 2r \le 2s+1. \qquad \text{(B5)}$$

$$[G_{*\circ}^{\text{TB}}(\tilde{E})]_{rs} = c_{rs}(\tilde{E}), r > s. \qquad \text{(B6)}$$

Turn now to the QCTB case. Using rule (A9), and Eqs. (9) and (10) we obtain ($r \le s$)

$$[G_{**}^{\text{TB}}(\tilde{E})]_{rs} = \frac{\tilde{E}}{\tilde{E}_\delta} a_{rs}(\tilde{E}_\delta), \qquad \text{(B7)}$$

and $[G_{**}^{\text{TB}}(E)]_{sr} = [G_{**}^{\text{TQCB}}(E)]_{rs}$. Likewise, we have the following QCTB analogues of Eqs. (B4)–(B6):

$$[G_{\circ\circ}^{\text{QCTB}}(E)]_{rs} = \frac{\tilde{E}}{\tilde{E}_\delta} a_{n-r+1,n-s+1}(\tilde{E}_\delta), r \le s, \qquad \text{(B8)}$$

$$[G_{*\circ}^{\text{QCTB}}(E)]_{rs} = b_{rs}(\tilde{E}_\delta), 2r \le 2s+1, \qquad \text{(B9)}$$

$$[G_{*\circ}^{\text{QCTB}}(\tilde{E})]_{rs} = c_{rs}(\tilde{E}_\delta), r > s. \qquad \text{(B10)}$$

For the simplest case of $E = 0$ and $\delta = 0$, we naturally reproduce the reported result from [21] (in our notation): $[G_{*\circ}^{\text{TB}}(0)]_{rs} = (-1)^{r-s}$, and $[G_{**}^{\text{TB}}(0)]_{rs} = [G_{\circ\circ}^{\text{TB}}(0)]_{rs} = 0$.

Let us briefly consider a more complicated problem pertaining to a polyene chain with alternated bond lengths. We present here only a partial solution, restricting ourselves by computations of the most interesting GF matrix elements between the first starred site and any unstarred site of the chain, that is a set $\{[G_{*\circ}^{\text{QCTB}}(E)]_{1,r}\}_{1 \le r \le n}$. As a start, consider the TB model for which the known Lennard-Jones results [43] about the Huckel spectrum in polyenes will serve as an initial point. To do this, one needs to additionally introduce the bond alternation into the TB Hamiltonian through a parameter τ defined in section 4. Using the corresponding TB Hamiltonian matrix and the secular determinant from [43], we get the required result by applying the standard technique of expanding determinant along rows:

$$[G_{*\circ}^{\text{TB}}(\tilde{E})]_{1,r} = (-\tau)^r d_{n-r}(\tilde{E})/d_n(\tilde{E}), \qquad \text{(B11)}$$

where

$$d_r(E) = \tau^{r-1}(1 - E^2)U_{r-1}[(\tau+1)/\tau - E^2/\tau)/2] -$$
$$- \tau^r U_{r-2}[(\tau + 1/\tau - E^2/\tau)/2].$$

The QCTB counterpart of this equation is made by replacing $\tilde{E} \to \tilde{E}_\delta$, as in Eq. (A9), thus giving

$$[G_{*\circ}^{QCTB}(\tilde{E})]_{1,r} = (-\tau)^r d_{n-r}(\tilde{E}_\delta)/d_n(\tilde{E}_\delta). \qquad \text{(B12)}$$

In particular, we can explicitly give Eq. (B11) for $E = 0$. After simple algebra we find:

$$[G_{*\circ}^{\text{TB}}(0)]_{1,r} = (-\tau)^{r-1}. \qquad \text{(B13)}$$

In transforming Eq. (B11) we used the known identity for $U_k((z + z^{-1})/2)$ (e. g., see Table B.2 in [44]). Expression (B13), is, of course, in a full agreement with the previously given TB result in [21]; for instance, the element $[G_{*o}^{TB}(0)]_{1,n}$ becomes exponentially small for sufficiently long chains, because $\tau \leq 1$.

Consider in further detail the butadiene example ($N = 4$) for which one can obtains the following matrix elements of interest at the QCTB level:

$$G_{1,4}^{QCTB}(E) = -(1 + \delta^2 - E^2)/\Delta_4, \quad (B14)$$
$$G_{2,3}^{QCTB}(E) = \tau(\delta^2 - E^2)/\Delta_4,$$

where we return to the usual site numeration as in Fig. (1); moreover, $\Delta_4 = (E^2 - \delta^2)^2 - (\tau^2 + 2)(E^2 - \delta^2) + 1$. In the context of quantum interference this example is discussed in section 4.

References

1. J.C.Cuevas, E.Scheer, Molecular Electronics: An Introduction to Theory and Experiment, World Scientific, Singapore (2010).

2. R.M.Metzger, *Chem. Rev.*, **115**, 5056 (2015).

3. Handbook of Single-molecule Electronics, ed. by K.Moth-Poulsen, Pan Stanford Publishing Pte. Ltd, Singapore (2016).

4. D.Xiang, X.Wang, C.Jia et al., *Chem. Rev.*, **116**, 4318 (2016).

5. H.Haug, A-P.Jauho, Quantum Kinetics in Transport and Optics of Semiconductors, Springer, Berlin (1996).

6. E.N.Economou, Green's Functions in Quantum Physics, Springer-Verlag, New York (1979).

7. Y.Tsuji, E.Estrada, R.Movassagh, R.Hoffmann, *Chem. Rev.*, **118**, 4887 (2018).

8. G.C.Solomon, J.P.Bergfield, C.A.Stafford, M.A.Ratner, *Beilstein J. Nanotech.*, **2**, 862 (2011).

9. K.G.L.Pedersen, M.Strange, M.Leijnse et al,, *Phys. Rev. B*, **90**, 125413 (2014).

10. A.V.Luzanov, *Functional Materials*, **21**, 437 (2014).

11. A.V.Luzanov, in: Practical Aspects of Computational Chemistry IV, ed. by J.Leszczynski, M.K.Shukla, Springer, New York (2016), p.151–206.

12. A.V.Luzanov, F.Plasser, A.Das, H.Lischka, *J. Chem. Phys.*, **146**, 064106 (2017).

13. F.A.Bulat, S.-H.Ke, W.Yang, L.Couchman, *Phys. Rev. B*, **77**, 153401 (2008).

14. S.H.Ke, M.Yang, S.Curtarolo, H.U.Baranger, *Nano Lett.*, **9**, 1011 (2009).

15. C.J.O.Verzijl, J.S.Seldenthuis, J.M.Thijssen, *J. Chem. Phys.*, **138**, 094102 (2013).

16. N.Trinajstic, Chemical Graph Theory, CRC Press, Boca Raton, Florida (1992).

17. R.Bass, *J. Math. Phys.*, **26**, 3068 (1985).

18. G.Y.Hu, R.F.O'Connell, *J.Phys.A: Math. Gen.*, **29**, 1511 (1996).

19. C.M.da Fonseca, J.Petronilho, *Lin. Alg. and its Appl.*, **325**, 7 (2001).

20. N.Nemec, D.Tomanek, G.Cuniberti, *Phys. Rev. B*, **77**, 125420 (2008).

21. Y.Tsuji, R.Hoffmann, R.Movassagh, S.Datta, *J. Chem. Phys.*, **141**, 224311 (2014).

22. B.T.Pickup, P.W.Fowler, M.Borg, I.Sciriha, *J. Chem. Phys.*, **143**, 194105 (2015).

23. X.Zhao, V,Geskin, R.Stadler, *J. Chem. Phys.*, **146**, 092308 (2017).

24. E.G.Emberly, G.Kirczenow, *J. Phys.: Condens. Matter,*, **11**, 6911 (1999).

25. W.Barrett, *Linear Algebra Appl.*, **27**, 211 (1979).

26. Y.Tsuji, T.Stuyver, S.Gunasekaran, L.Venkataraman, *J. Phys. Chem. C*, **121**, 14451 (2017).

27. A.T.Amos, M.Woodward, *J. Chem. Phys.*, **50**, 119 (1969).

28. A.V.Luzanov, Y.F.Pedash, V.V.Ivanov, *J. Struct. Chem.*, **30**, 701 (1989).

29. A.V.Luzanov, E.N.Babich, V.V.Ivanov, *J. Mol. Struct. (Theochem)*, **311**, 211 (1994).

30. A.V.Luzanov, V.V.Ivanov, I.V.Boichenko, *J. Mol. Struct. (Theochem)*, **360**, 167 (1996).

31. D.M.Cardamone, C.A.Stafford, S.Mazumdar, *Nano Lett.*, **6**, 2422 (2006).

32. M.M.Mestechkin, *Zh. Fiz. Khim.*, **35**, 431 (1961); M.V.Basilevski, Molecular Orbitals Method and Reactivity of Organic Molecules, Khimia, Moscow (1969).

33. J.P.Malrieu, R.Caballol, C.J.Calzado et al., *Chem. Rev.*, **114**, 429 (2014).

34. E.H.Lieb, *Phys. Rev. Lett.*, **62**, 1201 (1989).

35. A.A.Ovchinnikov, *Theor. Chem. Acta*, **47**, 297 (1978).

36. A.E.Albert, Regression and the Moore-Penrose Pseudoinverse, Academic Press, New York (1972).

37. MATHEMATICA version 5.2, Wolfram Research, Inc. Champaign. Champaign, Illinois (2005).

38. A.V.Luzanov, *J. Struct. Chem.*, **25**, 837 (1985).

39. P.W.Fowler, B.T.Pickup, T.Z.Todorova, W.Myrvold, *J. Chem. Phys.*, **131**, 244110 (2009).

40. T.Morikawa, S.Narita, D.J.Klein, *Chem. Phys. Lett.*, **402**, 554 (2005).

41. T.Tada, K.Yoshizawa, *Chem.Phys.Chem*, **3**, 1035 (2002).

42. R.Sykora, T.Novotny, *J. Chem. Phys.*, **146**, 174114 (2017).

43. J.L.Lennard-Jones, *Proc. R. Soc. A*, **158**, 280 (1937).

44. J.C.Mason, D.C.Handscomb, Chebyshev Polynomials, Chapman&Hall, London (2003).

45. E.Estrada, *Proc. R. Soc. A*, **474**, 20170721 (2018).